

## Measurements of K-shell ionization cross sections of Cr, Ni and Cu by impact of 6.5–40 keV electrons

X Llovet†||, C Merlet‡ and F Salvat§

† Serveis Científico-Tècnics, Universitat de Barcelona, Lluís Solé i Sabarís 1-3, 08028 Barcelona, Spain

‡ ISTEEM, FU 160, CNRS, Université de Montpellier II, Sciences et Techniques du Languedoc, Place E Bataillon, 34095 Montpellier Cedex 5, France

§ Facultat de Física (ECM), Universitat de Barcelona, Societat Catalana de Física, Diagonal 647, 08028 Barcelona, Spain

E-mail: xavier@giga.sct.ub.es

Received 27 January 2000, in final form 5 May 2000

**Abstract.** Results from measurements of K-shell ionization cross sections of the elements Cr, Ni and Cu by electron impact with energies in the range 6.5–40 keV are presented. Cross sections were obtained by measuring characteristic x-rays emitted from (1–6 nm thick) films of the studied elements deposited on self-supporting carbon backing films. The procedure yields relative cross sections with uncertainties of the order of 2%. Transformation to absolute units increases the uncertainties to about 10%. Our results are compared with those from other groups and with two calculations based on the first Born approximation, which include corrections for exchange, Coulomb and relativistic effects. A simple empirical formula that accurately describes the energy dependence of the measured cross sections is provided.

### 1. Introduction

Accurate cross sections for inner-shell ionization by impact of keV electrons are required for quantitative analysis in Auger electron spectroscopy (AES), electron probe microanalysis (EPMA) and electron energy loss spectroscopy (EELS), as well as for many applications in other fields. Calculations of ionization cross sections within the plane-wave first Born approximation (PWBA) provide reliable results for high-energy electrons. Near the ionization threshold, however, the PWBA is not adequate due to the distortion caused by the atomic field to the incident and emerging waves and because of the effects of electron exchange. For elements of medium and high atomic numbers, relativistic effects must also be taken into account. Owing to the difficulties of calculations using more accurate (distorted-wave) methods, semi-empirical modifications of the PWBA have been proposed to account for the above-mentioned effects (Hippler 1990, Mayol and Salvat 1990). For practical purposes, a variety of empirical and semi-empirical formulae have also been proposed (see e.g. Powell 1985).

About ten years ago, available experimental cross sections for ionization of the K shell were compiled by Long *et al* (1990). Since then, additional measurements have been reported e.g. by Schneider *et al* (1993) and by a group of Chinese researchers (see Peng *et al* 1998 and

|| Corresponding author.

references therein). Inspection of the currently available experimental data reveals that they are still scarce for many elements and, when they are available, one usually finds significant discrepancies between data from different authors, which are often much larger than the stated experimental uncertainties. This reflects the fact that measurements of ionization cross sections face considerable experimental difficulties. In the case of measurements on solid targets (usually thin films), electron transport within the active film and in the substrate (when present) produces a spread in energy and direction of the beam, which must be properly accounted for. Results from relative measurements, which provide the dependence of the cross section  $\sigma_K$  on the energy  $E$  of the projectile, are affected by uncertainties arising from the energy spread of the incident electron beam, the counting statistics, possible instabilities etc. The transformation of the measured signal into absolute cross sections requires accurate knowledge of the target thickness, detector efficiency, solid angle of detection, number of incident electrons, fluorescence yield and line fractions. These quantities are nearly independent of the incident electron energy and, therefore, possible errors in the adopted values cause a global shift of the cross section versus energy curve without altering its 'shape'. Knowledge of an accurate 'relative' cross section (i.e. the function  $\sigma_K(E)$  apart from an indeterminate multiplicative constant) is useful for practical applications (e.g. in EPMA) and also to assess the reliability of empirical formulae and various semi-empirical corrections that have been proposed to extend the validity of the PWBA to energies near the ionization threshold.

In this paper, we report new measurements of K-shell ionization cross sections for elements Cr ( $Z = 24$ ), Ni ( $Z = 28$ ) and Cu ( $Z = 29$ ), from the corresponding ionization thresholds up to 40 keV. Special care has been exercised to determine the energy dependence of the cross section (i.e. the relative cross section), which has been measured by varying the electron incident energy in steps of 0.5–1 keV. Cross sections have been obtained from the characteristic x-rays emitted by thin films of the studied elements. The method is based on the use of (i) very thin active films, deposited on 30 nm thick carbon self-supporting films, (ii) a commercial electron microprobe with wavelength-dispersive x-ray spectrometers and a Si(Li) detector, (iii) a procedure for checking the absolute calibration of the instrument that combines results from Monte Carlo simulations with measured thick-target bremsstrahlung (TTB) spectra and (iv) an accurate method for determining film thicknesses based on the measurement of electron-induced x-ray intensities from equivalent films deposited on thick substrates. By combining all these factors, relative cross sections have been determined with uncertainties of the order of 2%; the corresponding absolute cross sections have uncertainties of about 10%.

Details on the experimental procedure and on the methods used to evaluate the data are given in section 2. In section 3 we compare our measured cross sections with experimental data from other authors and with predictions of two PWBA-based theoretical models, which include corrections for exchange, Coulomb and relativistic effects (Hippler 1990, Mayol and Salvat 1990). Finally, in section 4 we offer our conclusions.

## 2. Experimental method and data correction

To determine the K-shell ionization cross sections  $\sigma_K$  we measured the number of characteristic x-rays ( $N_{K\alpha}$ ) emitted from the specimen bombarded with  $N_e$  electrons of energy  $E$ . For a homogeneous film of thickness  $t$  and a normally incident electron beam, the K-shell ionization cross section can be expressed as (see e.g. Shima *et al* (1981))

$$\sigma_K(E) = \frac{1}{\omega_K} \frac{I_\alpha + I_\beta}{I_\alpha} \frac{4\pi}{N t N_e \epsilon \Delta\Omega} N_{K\alpha}(E), \quad (1)$$

where  $I_\alpha$  and  $I_\beta$  are the line fractions of the  $K\alpha$  and  $K\beta$  peaks,  $N_{K\alpha}(E)$  is the number of detected characteristic  $K\alpha$  x-rays,  $\mathcal{N}$  is the atomic target density (atoms per unit volume),  $\omega_K$  is the fluorescence yield,  $\Delta\Omega$  is the solid angle subtended by the spectrometer and  $\epsilon$  is the spectrometer efficiency. Notice that equation (1) assumes that electrons penetrate the film following a straight trajectory without losing energy. This implies that the thickness of the film must be small enough; for the energies and materials considered in the present work the active film must be so thin that it cannot support itself.

The studied samples were Cr, Ni and Cu thin films deposited on carbon self-supporting films and were produced as follows. Firstly, carbon films approximately 30 nm thick were thermally evaporated on mica films. Because of its low atomic number (small backscattering effect) and large tensile strength, carbon films are adequate to hold the active films. The mica films were separated from the carbon films in distilled water; carbon films floating on the water surface were removed with a grid of the kind used in transmission electron microscopy. Cr, Ni and Cu films were then deposited by thermal evaporation on the previously prepared carbon films. During the same evaporation runs, twin films of the studied element were deposited on thick polished ultra-pure GaAs and Si targets, to be used for thickness determination as described below. Electron micrographs and EPMA measurements did not show any indication of islanding of the evaporated metal.

The apparatus used for electron bombardment and for the detection of characteristic x-rays from the specimen was a Cameca SX-50 electron microprobe. A high-voltage generator provides the accelerating voltage of the beam generated by an electron gun, which is focused onto the target by means of an electromagnetic lens system. The final diameter of the beam on the target is several micrometres. The electron microprobe is equipped with a beam regulation device that ensures stability of the beam current ( $\sim 0.3\%$  maximum fluctuation during  $\sim 1$  h). Conventional high-vacuum technology is used to prevent breakdown of the accelerating voltage and scattering of electrons in the beam by residual atoms. Generated x-rays can be measured by a PGT IMIX energy-dispersive spectrometer, which uses a Si(Li) detector and by four wavelength-dispersive spectrometers. According to the manufacturer's specifications, the Si(Li) is 3 mm thick and has an active area of 12.5 mm<sup>2</sup> and there is a 7  $\mu$ m thick beryllium window placed in front of the detector. Each wavelength-dispersive spectrometer consists of a crystal monochromator and a gas proportional counter (gas-flow open type), with an argon-methane (90 : 10) mixture used as a counter gas and a separation window of Mylar and/or polypropylene. Both energy and wavelength-dispersive spectrometers are located along an axis that forms an angle of 40° with respect to the sample surface.

To determine the film thicknesses  $t$ , we measured the ratio of x-ray intensities (the so-called  $k$ -ratio) from the Cr/Si, Ni/GaAs and Cu/GaAs targets to the intensities of the same peaks measured on pure Cr, Ni and Cu targets (see e.g. Scott *et al* 1995). Measured  $k$ -ratios were analysed with the help of the X-FILM analysis code (Merlet 1995), which calculates the thicknesses and concentrations of a multilayer target by least-squares fitting of an analytical x-ray emission model to the experimental data (see figure 1). It should be stressed that when the atomic numbers of the layer and substrate are close (this is the case for the three considered specimens) the depth distribution of ionization in the film material is accurately described by using the corresponding part of the ionization distribution in the bulk material, which is relatively well known. The accuracy of the thickness estimation provided by the X-FILM code is then expected to be better than 6%. The estimated thicknesses of the active films were in the range from 1 to 6 nm.

Although the specimens (active film plus backing carbon layer) are very thin, incident electrons suffer some scattering and do not penetrate straight through them. The mean track length  $l_e$  of transmitted electrons is somewhat greater than the actual film thickness and,

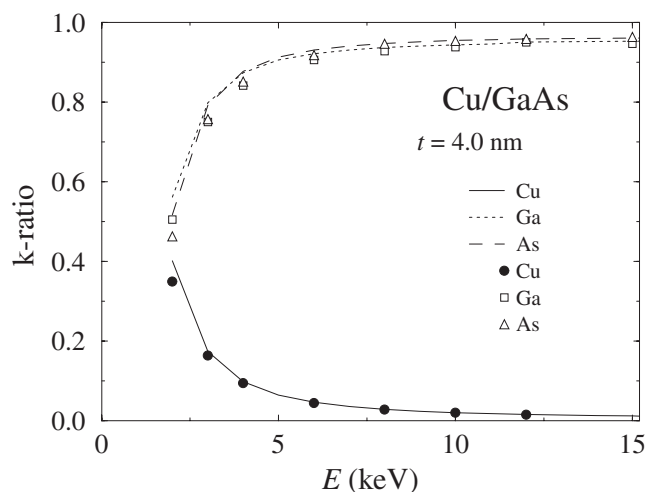


**Figure 1.** Value of the  $k$ -ratio for Cu  $L\alpha$ , Ga  $L\alpha$  and As  $L\alpha$  x-ray lines from a 4.0 nm thick film of Cu deposited on a GaAs substrate as a function of the electron incident energy. The  $k$ -ratio was determined with respect to pure Cu for the Cu  $L\alpha$  line, and with respect to pure GaAs for the Ga  $L\alpha$  and As  $L\alpha$  lines. Symbols represent experimental data. Curves are results from the x-ray emission model of Merlet (1995).

moreover, it depends on the incident electron energy. The mean track length of electrons that are transmitted through the metal film (with exit energies larger than the considered ionization threshold) was estimated by using the general-purpose Monte Carlo simulation code described by Baró *et al* (1995). Figure 2 displays the calculated fractional mean track lengths  $l_e/t$  of electrons transmitted through 5.2, 5.6 and 1.4 nm thick films of Cr, Ni and Cu, respectively. Differences between the real film thickness and the mean track length are seen to be less than  $\sim 4\%$  for the considered films. To account for the spread of the beam within the active film, the film thickness  $t$  in equation (1) was replaced by the energy-dependent electron mean track length  $l_e$  (as given in figure 2). On the other hand, electrons lose energy due to inelastic collisions within the film and, therefore, their 'effective' energy is somewhat smaller than the energy  $E$  of the incident beam. To estimate the effective energy, we calculated the average energy loss of electrons transmitted through the film, as a function of the incident energy, using a Monte Carlo simulation. For the samples and energies considered here, this energy loss was found to be less than 1.0% of the incident energy and it was neglected. In equation (1) we have disregarded the fact that electrons backscattered by the carbon backing can also produce ionizations in the active film. To evaluate the increase of the ionization probability due to this effect, we performed simulations of electron transport in the complete specimen (active film + carbon backing), combined with ionization cross sections  $\sigma_K(E)$  calculated from the hydrogenic optical data model of Mayol and Salvat (1990). For the Ni/C specimen, it was found that the increase in the number of ionizations ranged from  $\sim 0.6\%$  at 30 keV to  $\sim 0.1\%$  at 10 keV. Ionizations produced by the influence of the carbon backing were consequently neglected.

X-ray measurements were carried out using a wavelength-dispersive spectrometer for different beam energies spanning the range from the ionization threshold up to 40 keV, in steps of 0.5–1 keV. It is worth pointing out that the better resolution (and hence the better sensitivity) of a wavelength-dispersive spectrometer, as compared with a Si(Li) detector, makes it much more adequate for the measurement of low x-ray intensities, such as the

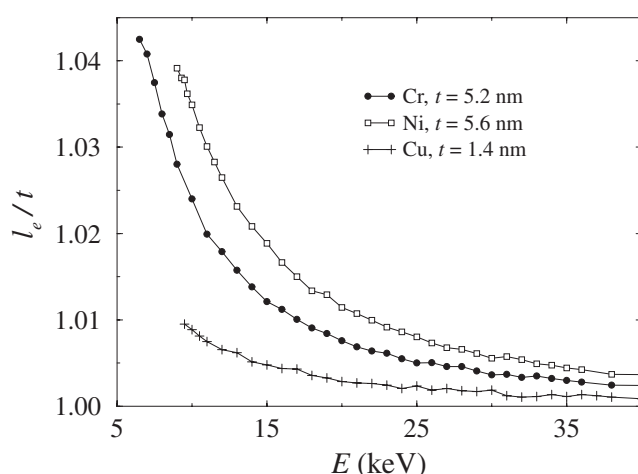


**Figure 2.** Simulated fractional track length  $l_e/t$  of electrons transmitted through self-supporting Cr, Ni and Cu films of the indicated thicknesses, as a function of the incident electron energy (see the text). Simulated results are represented by symbols, joined by straight segments for visual aid.

ones yielded by the extremely thin films used in our experiments. This fact makes the wavelength-dispersive spectrometer an ideal device for determining ionization cross sections near the ionization threshold. The high-energy part of the corresponding energy-dispersive x-ray spectrum (bremsstrahlung tip) was used to check the value of the accelerating potential. Electron currents were selected to meet a certain compromise between x-ray counting rate and film damage, with typical values of 100 nA. Measurements were performed on the wavelength channel corresponding to the maximum of the characteristic peak, using a lithium fluoride (LiF) crystal. Bremsstrahlung background was subtracted by linear interpolation of the spectral background on both sides of the peak. Counting times were about 100 s for each peak and 50 s for the background. For each beam energy and sample, at least ten measurements were performed at different positions on the sample. Therefore, the standard deviation for the set of measurements accounts not only for uncertainties due to counting statistics, but also for errors arising from possible inhomogeneities in the active film thickness. Relative uncertainties due to counting statistics, sample non-uniformity, background subtraction and beam spreading (in both energy and direction of motion), for an incident beam energy near the maximum of the ionization cross section curve, are estimated to be  $\sim 2\%$ .

In the present work, we use fluorescence yields  $\omega_K$  taken from the tabulation of Hubbell *et al* (1994); for the elements of interest, they have uncertainties of about 2–3%. The adopted values of the line fractions  $I_\alpha$  and  $I_\beta$  are the most probable values reported by Khan and Karimi (1980), which were derived from a compilation of available experimental data and which are found to agree satisfactorily (within less than 2%) with the line fractions observed in our measured spectra. Explicitly, the values used in the present work are the following:

$$\begin{aligned}
 \text{For Ni,} \quad \omega_K &= 0.412, & [I(\alpha) + I(\beta)]/I(\alpha) &= 1.136. \\
 \text{For Cu,} \quad \omega_K &= 0.441, & [I(\alpha) + I(\beta)]/I(\alpha) &= 1.137. \\
 \text{For Cr,} \quad \omega_K &= 0.286, & [I(\alpha) + I(\beta)]/I(\alpha) &= 1.133.
 \end{aligned}$$

The absolute efficiency of a wavelength-dispersive spectrometer is the product of the crystal reflection efficiency and the proportional counter efficiency. The crystal reflection efficiency, i.e. the fraction of x-rays reflected on the crystal, depends on both the geometry

and the properties of the crystal (dislocations, surface texture, stress, stability and thermal expansion). The efficiency of the proportional counter depends on the detector window and the fraction of the incident x-rays absorbed in the counter itself. On the other hand, the solid angle subtended by the crystal changes as it moves. As a result, the absolute efficiency of a wavelength-dispersive spectrometer is a complicated function of the incident photon wavelength (Reusch *et al* 1986) and it is difficult to determine. To overcome this difficulty we used the Si(Li) detector of the microprobe. The absolute efficiency of a Si(Li) detector is the product of its intrinsic efficiency and the collection solid angle. Assuming that the intrinsic efficiency is equal to unity, which is plausible for photons with energies in the interval from  $\sim 3$  to 15 keV (see e.g. Paterson *et al* 1989), the absolute efficiency is directly determined by the collection solid angle. X-ray measurements from each specimen were therefore performed for selected energies and for various positions of the incident beam by using the Si(Li) detector (see below) and converted into absolute cross section values following equation (1). A 'scaling' factor was then obtained by taking the ratio of these absolute cross section values to the corresponding x-ray intensities (measured with the wavelength-dispersive spectrometer). Thus, multiplication by the scaling factor converts the relative cross sections into absolute units. The standard deviation of the scaling factors was typically less than 2%.

In the measurements with the Si(Li) detector, beam currents were chosen to yield dead-time counting losses lower than 1–2%. Probe currents were measured with a Faraday cup placed on the sample holder, and the number of incident electrons  $N_e$  was evaluated by multiplying the probe current  $I_0$  by the 'live' acquisition time, determined by the PGT IMIX software. Measurement times were typically about 4000 s/spectrum, which ensures that the statistical uncertainty of the x-ray peaks is less than 2%. Peak intensities were obtained by measuring the area of the corresponding peak after subtracting the background by using a polynomial fit. To minimize stray radiation from elsewhere in the specimen chamber, the emerging photon beam was collimated with a 0.3 mm diameter diaphragm placed in front of the beryllium window, at 53 mm from the specimen. Also, a small Faraday cup (2 mm diameter aperture) was placed below the target, aligned to the impact point of incident electrons, with the aim of absorbing most of the transmitted electrons. To make sure that stray radiation does not contribute to the peaks of interest, x-ray spectra were collected within a 'blank' target, i.e. a self-supporting carbon film with no active film attached, at different electron incident energies. These spectra showed no significant peaks at the energies of interest.

In order to check the reliability of the 'absolute' calibration of our measurements, i.e. the conversion of measured x-ray intensities in counts per second per unit electron current into counts per incident electron per unit solid angle (which involve the product of the determined absolute efficiency and number of incoming electrons), x-ray spectra were acquired on thick targets with the Si(Li) detector and converted into an absolute scale. The absolute spectrum  $N(E_{\text{ph}})$  (i.e. normalized to give the number of emitted photons per unit energy, per unit solid angle, per incident electron) was determined from the relation  $N(E_{\text{ph}}) = [N_{\text{ch}}(E_{\text{ph}})/N_e \epsilon \Delta \Omega \Delta E_{\text{ph}}]$ , where  $N_{\text{ch}}$  is the number of counts in an energy channel about  $E_{\text{ph}}$  of the measured spectrum,  $\Delta E_{\text{ph}}$  is the channel width and  $N_e$  is the number of incoming electrons. TTB spectra were calculated by using the Monte Carlo simulation model developed by Acosta *et al* (1998). Briefly, the simulation of bremsstrahlung emission is based on an analytical cross section model which yields stopping powers and angular distributions of emitted photons in good agreement with the calculations of Kissel *et al* (1983). Absolute spectra simulated with this code have been shown to agree closely with experiments (Acosta *et al* 1998, Llovet *et al* 2000). The agreement between experimental and calculated TTB spectra was found to be satisfactory (within  $\sim 6\%$ ) for the studied elements. As an example, figure 3 displays simulated and measured absolute spectra of x-rays from Ni under 20 keV

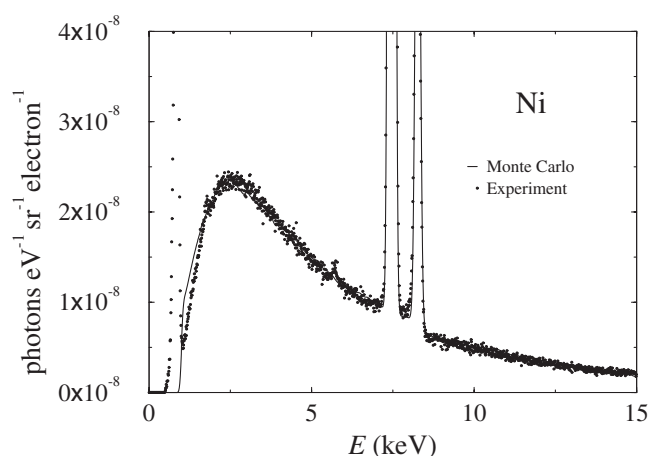


**Figure 3.** Simulated (solid curve) and experimental (symbols) TTB spectra from pure Ni generated by 20 keV electrons at normal incidence.

electron bombardment. This procedure provides a direct verification of the absolute calibration of our instrument, and allows us to estimate its uncertainty at  $\sim 6\%$ .

Experimental measurements are affected by two different kinds of error. Those of the first kind, referred to as relative uncertainties, arise from counting statistics, background subtraction, sample non-uniformity and instrumental drift during measurements. They are different for each incident electron energy and, therefore, they affect the relative shape of the cross section curve. The magnitude of these relative uncertainties has been estimated to be 2%. The conversion of the relative cross sections to absolute values introduces other kinds of error, of a systematic nature. These originate from uncertainties in the determination of film thicknesses (6%), absolute calibration of the instrument (6%), the scaling factor (2%), fluorescent yields (2–3%) and line fractions (2%). The estimated global uncertainties, obtained by combining relative uncertainties and systematic errors in quadrature, are about 10%.

### 3. Results and discussion

The results of our measurements are given in table 1. As mentioned above, the associated global uncertainties are of the order of 10%. Notice, however, that the shape of the cross section curve (i.e. the relative cross section values) is much more accurate ( $\sim 2\%$ ), since it is only affected by relative uncertainties.

It is of interest to compare our results with the predictions of simple theoretical models. We shall consider the plane-wave Born calculation described by Hippler (1990), which uses a simple Coulomb correction to take into account the distortion of the projectile wavefunctions by the atomic field and incorporates exchange effects through the Ochkur correction. For ionization of K shells, the generalized oscillator strength is evaluated by using a hydrogenic model, which leads to an analytical expression for the double differential cross section (differential in the energy loss and scattering angle of the projectile), which can be easily integrated to obtain the ionization cross section. We shall also consider a similar model proposed by Mayol and Salvat (1990), which is based on a simple representation of the generalized oscillator strength obtained from knowledge of the (dipole) cross section for photoelectric absorption of photons in the considered atomic shell. The model also

**Table 1.** Measured absolute K-shell ionization cross sections for Cr, Ni and Cu. The absolute uncertainties are about 10%.

Energy (keV)	Cr cross section (barn)	Ni cross section (barn)	Cu cross section (barn)
6.5	143		
7	283		
7.5	393		
8	485		
8.5	556		
9	606	77	
9.3		115	
9.5		134	52
9.7		156	
10	721	181	102
10.5		220	144
11	796	262	182
11.5		284	
12	856	313	244
13	880	357	294
14	913	396	332
15	920	427	362
16	946	452	382
17	953	472	405
18	970	482	420
19	967	497	438
20	967	504	448
21	970	507	453
22	966	511	460
23	970	523	465
24	965	520	474
25	940	532	487
26	958	530	484
27	938	531	493
28	952	526	493
29	932	528	488
30	922	533	494
31	918	526	492
32	911	526	491
33	896	526	490
34	897	528	484
35	899	526	484
36	874	523	486
37			479
38	848	518	483
40	832	514	482

incorporates exchange corrections, through the Ochkur approximation, and an empirical Coulomb correction.

Figure 4 displays absolute K-shell ionization cross sections measured in the present work, for solid Cr, Ni and Cu as functions of the incident electron overvoltage,  $u = E/E_K$ , where  $E_K$  is the K-shell ionization energy of the element. K-shell ionization cross sections predicted by the Hippler (1990) and Mayol and Salvat (1990) models are shown as solid and long-dashed

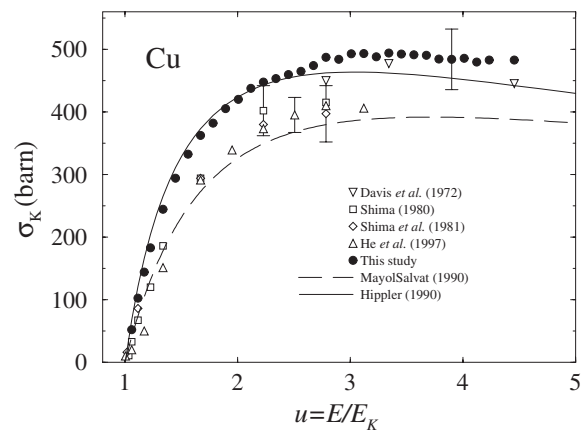
curves, respectively. Also displayed are results available from measurements by other authors. In the case of Cu (figure 4(c)), our results (solid circles) are in relatively good agreement with those of Davis *et al* (1972) and slightly higher (about 10%) than those of Shima (1980), Shima *et al* (1981) and He *et al* (1997). For Ni, available experimental data seem to form two groups; the results of Pockman *et al* (1947) and He *et al* (1997) are about 30% lower than the data of Jessenberg and Hink (1975) and Luo *et al* (1996). Our results (solid circles) are in good agreement with the second group of data. A similar trend is found for Cr (figure 4(c)); our measured cross sections agree well with the data reported by Luo *et al* (1996) and lie systematically higher (30%) than the measurements of He *et al* (1997). It is worth stressing that, in general, the discrepancies observed between data from different (and sometimes the same) groups are systematically larger than the claimed absolute uncertainties, which have been indicated in the figures for the cases where they were available. These inconsistencies make it difficult to assess the reliability of calculated cross sections on the basis of available experimental data and show the need for new, more systematic measurements of absolute ionization cross sections.

Regarding the comparison with the theoretical models of Hippler (1990) and Mayol and Salvat (1990), our data for Cu, as well as those from measurements of Davis *et al* (1972), agree with Hippler's (1990) model with differences that are of the same order of magnitude as the absolute experimental uncertainties. For Ni, Hippler's (1990) model seems to agree with our experimental results better than those of Mayol and Salvat (1990); near the ionization threshold Hippler's (1990) model departs increasingly from our measurements. For Cr, both models fall within the error interval of the experimental result. Agreement of Hippler's (1990) model with experiments for carbon, neon, argon and nickel atoms has also been reported by Khare *et al* (1993).

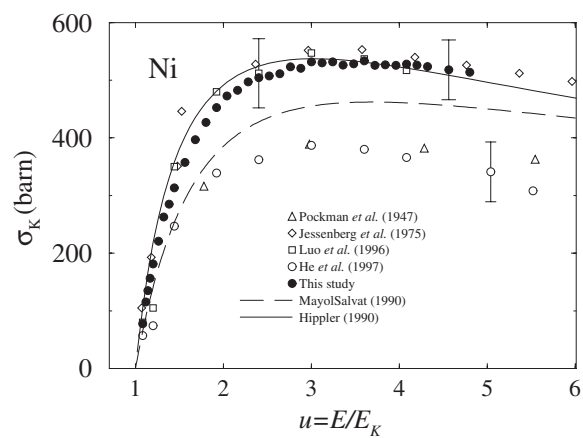
As mentioned above, our measurements provide the energy dependence of the ionization cross section with a much better accuracy (about 2% error) than that of the absolute cross section. In figure 5 we compare our measured (relative) cross sections for Ni with the predictions of the theoretical models of Hippler (1990) and of Mayol and Salvat (1990). The experimental data and the theoretical curves have been rescaled, with their maximum values set equal to unity, to show differences in 'shape'. Similar trends are observed for Cr and Cu. The results of the calculations of Hippler (1990) and Mayol and Salvat (1990) differ from our experimental data, but the differences (after normalization to unit maximum) are usually less than about 5%. This kind of comparison clearly reveals the limitations of simple PWBA-based models for small overvoltages. The continuous curve in figure 5 represents the function

$$\sigma_K(u)/\sigma_K^{\max} = \left( A_1 + \frac{A_2}{u} \right) \frac{1}{u^{A_3}} \ln(u), \quad (2)$$

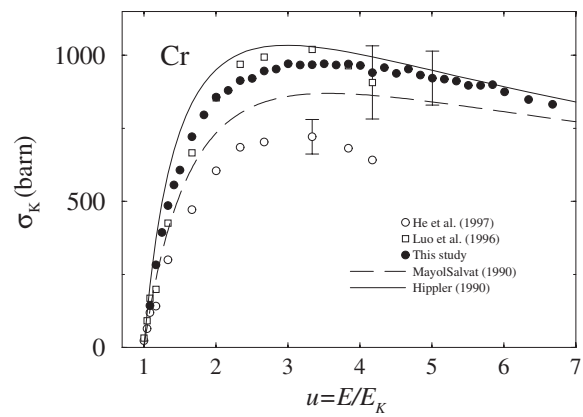
where  $\sigma_K^{\max}$  is the maximum value of the cross section and  $A_1$ ,  $A_2$  and  $A_3$  are parameters which are determined by numerical fit to the experimental data. The parameter values obtained for the three studied elements and the energy range where the fit applies are given in table 2. From this table, we see that there is a small, but not negligible, dependence of the parameters  $A_1$ ,  $A_2$  and  $A_3$  on the atomic number of the element. For practical purposes, however, it is of interest to provide a simple parametrization of the measured cross section data. By using the above function (2) with average values of the parameters given in table 2, i.e.  $A_1 = 2.36$ ,  $A_2 = -0.22$  and  $A_3 = 0.85$ , the measured cross sections are described with fairly good accuracy (see figure 6). The spread of the experimental data about this curve again confirms the claimed accuracy of our (relative) measurements.



(a)



(b)



(c)

**Figure 4.** K-shell ionization cross section versus overvoltage  $u$  for Cu (a), Ni (b) and Cr (c). The dashed curves indicate the calculation results from the model of Mayol and Salvat (1990), continuous curves indicate calculations according to Hippler's (1990) model. Full circles are results from the present measurements. Other symbols represent measurements by the authors indicated in the legends.

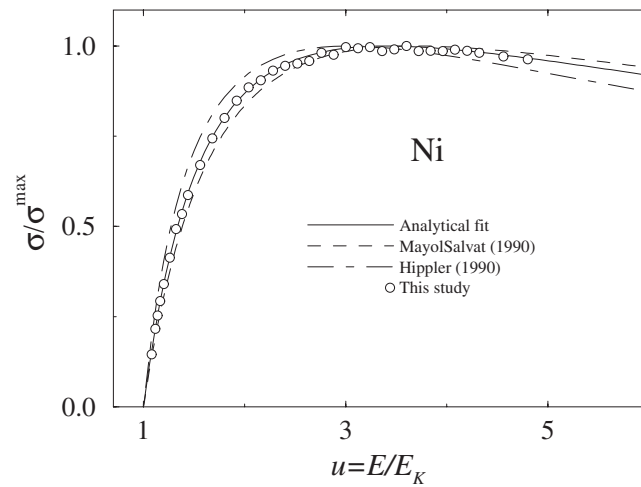


**Figure 5.** Experimental relative cross sections and calculated ionization cross sections (normalized to unit maximum value) for Ni as a function of the overvoltage  $u$ . The continuous curve is the function given by equation (2), with the parameter values indicated in table 2; the dashed curve is from the calculation of Mayol and Salvat (1990); the dot-dashed curve is from Hippler's (1990) calculation. Circles indicate results from the present measurements.

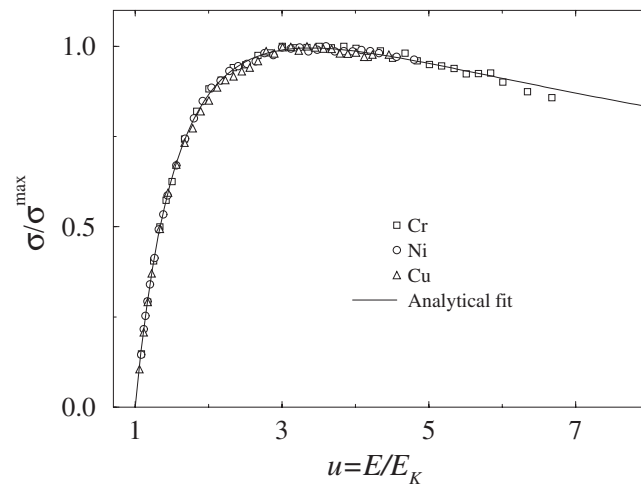


**Figure 6.** Relative cross section as a function of the overvoltage  $u$ . Symbols represent measured values for the indicated elements. The continuous curve is the function given by equation (2), with the parameter values indicated in the text.

**Table 2.** Parameters obtained from the fit of equation (2) to the relative cross section.

Element	$A_1$	$A_2$	$A_3$	Range of $u$
Cr	2.54	-0.39	0.90	1.08-6.67
Ni	2.31	-0.17	0.84	1.08-4.80
Cu	2.23	-0.11	0.81	1.05-4.45

#### 4. Conclusion

In conclusion, we have performed measurements of K-shell ionization cross sections for the elements Cr, Ni and Cu, from threshold up to 40 keV. The adopted experimental procedure and evaluation methods allowed us to reduce the relative and absolute uncertainties to about 2 and 10%, respectively. The PWBA-based models of Hippler (1990) and Mayol and Salvat (1990) predict the observed energy dependence of the ionization cross section to within 5%. Accurate relative measurements are of fundamental importance to check the accuracy of these and other, more involved, theoretical models (e.g. based on the distorted-wave Born approximation). Work to extend the measurements to other elements and to outer atomic shells is in progress.

#### Acknowledgments

We are indebted to Dr J M Fernández-Varea for fruitful discussions and for providing the PWBA calculations for figures 4 and 5. This work has been partially supported by Comisión para la Investigación Científica y Técnica (Spain), project no PB95-0271-C02-01. Financial support from the PICASSO programme (Acciones Integradas entre España y Francia), project HF1997-0033, is gratefully acknowledged.

#### References

- Acosta E, Llovet X, Coleoni E, Riveros J A and Salvat F 1998 *J. Appl. Phys.* **83** 6038  
Baró J, Sempau J, Fernández-Varea J M and Salvat F 1995 *Nucl. Instrum. Methods B* **100** 31  
Davis D V, Mistry V D and Quarles C A 1972 *Phys. Lett. A* **38** 169  
He F Q, Peng X F, Long X G, Luo Z M and An Z 1997 *Nucl. Instrum. Methods B* **129** 445  
Hippler R 1990 *Phys. Lett. A* **144** 81  
Hubbell J H, Trehan P N, Singh N, Chand B, Mehta D, Garg M L, Garg R R, Singh S and Puri S 1994 *J. Phys. Chem. Ref. Data* **23** 339  
Jessenberg J and Hink W 1975 *Z. Phys. A* **275** 331  
Khan M R and Karimi M 1980 *X-Ray Spectrosc.* **9** 32  
Khare S P, Saksena V and Wadehra J M 1993 *Phys. Rev. A* **48** 1209  
Kissel L, Quarles C A and Pratt R H 1983 *At. Data Nucl. Data Tables* **28** 381  
Llovet X, Valovirta E and Heikinheimo E 2000 *Mikrochim. Acta* **132** 205  
Long X, Lu M, Ho F and Peng X 1990 *At. Data Nucl. Data Tables* **45** 353  
Luo Z M, An Z, He F, Li T, Long X and Peng X 1996 *J. Phys. B: At. Mol. Opt. Phys.* **29** 4001  
Mayol R and Salvat F 1990 *J. Phys. B: At. Mol. Opt. Phys.* **23** 2117  
Merlet C 1995 *Proceedings on Microbeam Analysis* ed E S Etz (New York: VCH) p 203  
Paterson J H, Chapman J N, Nicholson W A P and Titchmarsh J M 1989 *J. Microsc.* **154** 1  
Peng X, He F, Long X, Luo Z and An Z 1998 *Phys. Rev. A* **58** 2034  
Pockman L T, Webster D L, Kirkpatrick P and Harworth K 1947 *Phys. Rev.* **71** 330  
Powell C J 1985 *Electron Impact Ionization* ed T D Märk and G H Dunn (Wien: Springer)  
Quarles C and Semaan M 1982 *Phys. Rev. A* **26** 3147  
Reusch S, Genz H, Löw W and Richter A 1986 *Z. Phys. D* **3** 379  
Schneider H, Tobehn I, Ebel F and Hippler R 1993 *Phys. Rev. Lett.* **71** 2707  
Scott V D, Love G and Reed S J B 1995 *Quantitative Electron-Probe Microanalysis* (New York: Ellis Horwood)  
Shima K 1980 *Phys. Lett. A* **77** 237  
Shima K, Nakagawa T, Umetani K and Mikumo T 1981 *Phys. Rev. A* **24** 72